2023 IEEE International Conference on Robotics and Automation (ICRA 2023)
May 29 - June 2, 2023. London, UK

A Handheld Hydraulic Cardiac Catheter with Omnidirectional Manipulator and Touch Sensing

Chi Cong Nguyen[1], James Davies[1], Mai Thanh Thai[1], Trung Thien Hoang[1], Phuoc Thien Phan[1], Kefan Zhu [1], Dang Bao Nhi Tran [2], Van Anh Ho [3], Hung Manh La [4], Hoang-Phuong Phan[5], Nigel H. Lovell[1], and Thanh Nho Do [1,*]

***Abstract*—Atrial fibrillation (AF) is mostly treated via robotic catheter-based cardiac ablation procedures. Over the last few decades, cables or tendon mechanisms are at the core of available cardiac catheters. Despite advances, the use of cables often results in considerable force loss, nonlinear hysteresis, and control challenges. Most catheters are not equipped with force sensing, which increases the risk of the ablation process and decreases their efficacy in clinical settings. In addition, current catheters have a poor user interface and therefore the ablation process requires skilled or trained surgeons to steer the complex motion of the catheter tip within the heart chambers. To improve the cardiac ablation procedure, a new robotic catheter that has the ability to extend its working space without moving its flexible body and a real-time force sensor for safe operation is highly desired. In this work, a new handheld and soft robotic catheter for AF ablation is introduced. The new device consists of several improved components such as a soft manipulator for navigation and bending motion, an ergonomic handheld controller, and a soft force sensor for monitoring tool-tissue contact. The design, modeling, and fabrication of the device are presented and followed by experimental characterizations and *ex-vivo* validation.**

***Index Terms*—Soft robotics, surgical catheter, soft robotic catheter, cardiac ablation, minimally invasive surgery**

I. Introduction

Heart arrhythmias or irregular heartbeats often result in severe patient morbidity and mortality as well as high monetary expenditures. One highly prevalent arrhythmia is atrial fibrillation (AF). Catheter ablation is normally used to remove aberrant electrical pathways and restore normal heart rhythm [1], [2]. Beyond the radiofrequency delivery, procedure strategy, imaging, and mapping state-of-the-art for enhanced safety and clinical outcome, better design for existing cardiac catheters is also critical [3]. Nonetheless, current catheter systems are having poor actuation methods (e.g., cables that are associated with high nonlinearities and force loss), lack tool-tissue contact information, and are complex to control [1], [4]. Consequently, it is essential to give surgeons a straightforward handheld robotic catheter with essential enhancements in terms of mechanical parts: (i) a bending manipulator with excellent dexterity and extensibility without the need of moving the flexible body; (ii) a comfortable and straightforward handheld controller; and (iii) a force sensor that can provide contact between the tissue and the catheter.

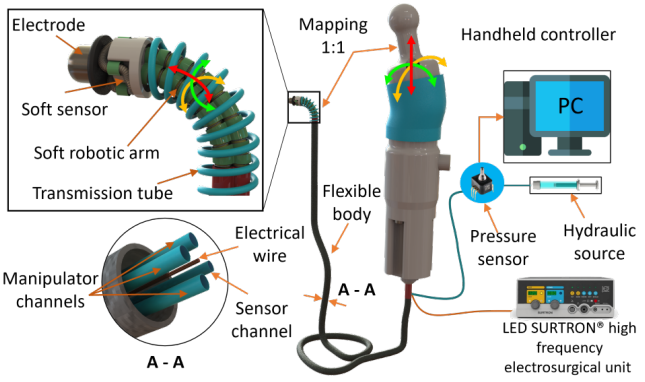

Fig. 1. Overview of the handheld soft robotic catheter device for cardiac ablation.

A wide range of actuation methods has been used to induce bending motion for the catheter tip. They include cable-driven actuators [5], [6], magnetic actuators [7], [8], electroactive polymers, and shape memory alloy (SMA) actuators [9]. Magnetic actuators require a bulky magnetic source and have low force. Other actuators are frequently linked to significant nonlinear friction or force loss, such as cable-driven actuators, or low-produced force and speed such as electroactive polymer or SMA actuators. Surgical robots and medical devices have benefited from recent improvements in soft fluidic actuators (SFAs) [10]–[14]. Driven by pressurized hydraulic fluids, they have the potential to overcome these difficulties due to their great conformability,

[1]The authors are with the Graduate School of Biomedical Engineering, Faculty of Engineering, UNSW Sydney, Kensington Campus, NSW 2052, Australia. (email: cong.c.nguyen@unsw.edu.au; j.j.davies@student.unsw.edu.au; maithanh.thai@unsw.edu.au; trungthien.hoang@unsw.edu.au; phuoc_thien.phan@unsw.edu.au; kefan.zhu@student.unsw.edu.au; n.lovell@unsw.edu.au; tn.do@unsw.edu.au)

[2]The author is with the School of Science, Engineering & Technology, RMIT University, Vietnam Campus, Ho Chi Minh City, Vietnam (email: s3751881@rmit.edu.vn)

[3]The author is with the School of Material Science, Japan Advanced Institute of Science, and Technology (JAIST), Ishikawa, Japan Science and Technology Agency, PRESTO, Kawaguchi Saitama, Japan (email: van-ho@jaist.ac.jp)

[4]The author is with the Department of Computer Science and Engineering, University of Nevada, Reno, Reno, NV 89557 USA (email: hla@unr.edu)

[5]The author is with the School of Mechanical and Manufacturing Engineering, Faculty of Engineering, UNSW Sydney, Kensington Campus, NSW 2052, Australia (email: hp.phan@unsw.edu.au)

[*]Coressponding author: T. N. Do (tn.do@unsw.edu.au)

dexterity, and ability to create high force and movement speed. However, achieving submillimeter-scale requirements for working against small and dexterous paths such as blood vessels without sacrificing the generated force is one of the main challenges.

It has been demonstrated that the precision of cardiac procedures is much improved with the availability of force information between the tool and tissue contact [15]. Previous studies have attempted to use different sensing technologies for medical devices such as piezoresistive technologies [16], [17], optical technologies (e.g., Fiber Bragg Gratings (FBGs) [18]), pressure sensors [19], [20], and magnetic technologies [21]. Despite significant progress, these sensing technologies are still associated with dimensional and geometrical constraints such as difficulties to integrate into the catheter tip, small bending angles, incompatible materials, low sensor resolution, and high hysteresis [2]. It is worth noting that the sensor size has a great effect on the catheter size [22].

For surgical robotic tools, the handheld paradigm has been successfully applied. Two examples include a handheld interface for da Vinci instruments [23] and an articulated endoscopic robot for natural orifice surgery [24]. More recently, the combination of a handheld controller with a robotic catheter has been introduced [13], [25]. However, none of them have an intuitive design, simple operation, and the ability to effectively control the robotic catheter with omnidirectional movements.

This paper presents a novel miniaturized and handheld soft robotic catheter with an omnidirectional flexible manipulator, a handheld controller, and a soft force sensor. The flexible manipulator and the force sensor were developed based on soft microtubule muscles (SMMs) [26] that can provide extension and contraction using hydraulic pressure. We selected hydraulic fluid rather than the pneumatic method to avoid the high compressibility of air, which is normally associated with slow response, high nonlinear hysteresis, and high noise. The handle, meanwhile, was quickly fabricated with an ergonomic-towards design. Through experimental characterizations and a diathermy experiment, the new catheter system's validity was also examined.

II. Design and Fabrication of the Catheter Device

A. Overview of the handheld soft robotic catheter device

The proposed device (Fig. 1) consists of a flexible bending manipulator, a catheter tip with an integrated soft sensor, a long flexible body, and an ergonomic handheld controller. The flexible manipulator is made of three separate Ø1.5 mm SMMs [26], capable of elongating and bending omnidirectionally to steer the catheter tip (see Fig. 1). Using soft hydraulic actuation for the flexible manipulator not only offers an effective method for robot dexterous navigation but also generates sufficient ablation force to be used in ablation procedures without scarifying its length. As a result, the flexible body can have a customizable length of at least 1000 mm. To drive the manipulator, the handheld controller is designed using a swashing mechanism with a fit-in-hand size of Ø25 mm. The integrated soft sensor (Ø0.8 x 8 mm) is highly sensitive (≈10.7 kPa/N), disposable, and fast and low-cost fabricated; and used to detect the contact force between the catheter tip and the heart tissue where the contact signals can be recorded as pressure data.

B. Flexible bending manipulator

We utilized three SMMs and medical heat shrink (Polyolefin, heat shrink ratio of 2:1) reinforcements (HSR) to create a 3-degrees of freedom (DOF) flexible manipulator. Each SMMs (Ø1.5 mm) was arranged in 120° apart (Fig. 2A. Two different sizes of the HSR were used: the longer one (red) covered the junction area between the transmission tube and the muscle while the shorter HSRs (green) were arranged along the active bending segment of the manipulator to enable omnidirectional manipulation and elongation of the catheter tip. In addition, the use of such a design significantly increased the stiffness and the generated force of the flexible manipulator.

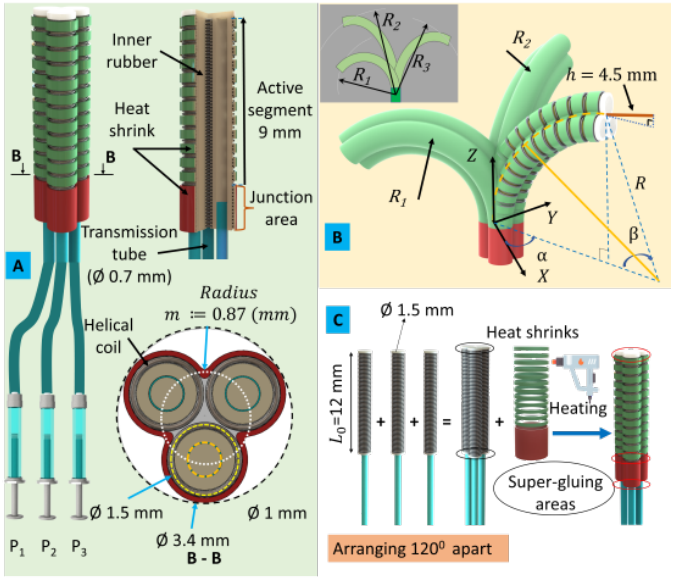

Fig. 2. (A) The design of the manipulator connected to its hydraulic sources with a quarter cut view and cross-section B-B; (B) Geometry parameters of the bending manipulator for modeling; (C) Fabrication process of the flexible manipulator.

The fabrication process for the flexible manipulator is shown in Fig. 2C. Briefly, three SMMs (each has an outer diameter of 1.5 mm and an initial length of 12 mm) were arranged 120° apart and fixed by adhesive glue together at their junction areas. It is noted that the sizes were chosen to provide a balance between flexibility, stability, and the ability to generate sufficient force, while also being compact enough to fit within the constraints of the catheter design. A red-color polyolefin heat shrink was then inserted into the junction area and heated by a heat gun. The next step involved heating a green heat shrink and stacking it on top

of the red heat shrink. This process was continued until the desired length was achieved. The green heat shrink covers a 9 mm-long active bending portion of the manipulator. The ultimate diameter of the manipulator was approximately 3.4 mm.

To determine the length of the SMM and its applied pressure, the relationship between input hydraulic pressure and SMM elongation is described as:

$$P_i = \frac{k_c l_i^2 + (k_c L_0 + EA_{tube}) l_i}{EA_{tube}} \tag{1}$$

where: L_0 (mm) is the initial active length of the bending segment, E (MPa) is Young's modulus of the soft micro-tubule material, A_tube (mm^2) is the cross-sectional area of the microtubule before applied fluid pressure, and k_c (N/mm) the spring constant of the helical coil. Details for these parameters can be found in [26].

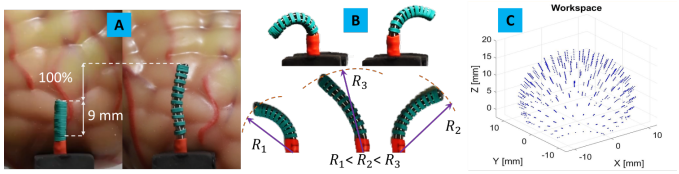

Fig. 3. (A) The flexible manipulator elongates at least 100% of its initial length and (B) performs workspace extension to reach different areas ($R_1 < R_2 < R_3$) without moving the catheter flexible body; (C) MATLAB simulation for the workspace of the catheter tip.

Under input pressure $P_i (i = 1, 2, 3)$, each SMM reaches the length of $L_i = L_0 + l_i$, where $l_i (i = 1, 2, 3)$ (mm) is its elongated length. As shown in Fig. 3, the flexible manipulator could extend to at least 100% of its initial length and also perform workspace extension without moving the catheter body, which contradicts the conventional cable-driven catheters where the external translation is required.

TABLE I
SPECIFICATIONS OF THE FLEXIBLE MANIPULATOR

Parameters	Symbol	Value
Helical coil: Stainless steel (Asahi Intecc Co., Ltd., Japan)		
Initial active length	L_0	9 mm
Helical coil stiffness	k_c	0.035 N/m
Microtubule: Silicone rubber (Saint-Gobain S.A., France)		
Cross-sectional area	A_{tube}	0.24 mm^2
Young's modulus of microtubule	E (100%)	1.648 MPa

It is noted that the manipulator would elongate along its neutral axis when $P_1 = P_2 = P_3$. By contrast, when there were any differences between these input pressures, the manipulator would bend. To predict the workspace of the catheter tip end effector, an analytical model was established based on the variation in the SMM lengths. The mapping between manipulator space and configuration space (see Fig. 2B) is depicted as follows:

$$R = \frac{(3L_0 + l_1 + l_2 + l_3)m}{2\sqrt{l_1^2 + l_2^2 + l_3^2 - l_1 l_2 - l_2 l_3 - l_3 l_1}} \tag{2}$$

$$\alpha = \tan^{-1}\left[\frac{\sqrt{3}(l_3 - l_2)}{l_2 + l_3 - 2l_1}\right] \tag{3}$$

$$\beta = \frac{2\sqrt{l_1^2 + l_2^2 + l_3^2 - l_1 l_2 - l_2 l_3 - l_3 l_1}}{3m} \tag{4}$$

where $R \in [0, \infty)$ is the radius curvature of the flexible manipulator; α is the angle of the bending plane concerning the X-axis, $\beta \in [0, 2\pi)$ is the bending angle of the arc of the manipulator, and m = 0.87 mm is the radius of the circle lying on the top plane that passes across the SMM neutral axis.

Since the catheter tip was attached to this top plane of the flexible manipulator, the distance from the end effector of the catheter tip to this plane h = 4.5 mm must be added (Fig. 2B). As such, the workspace of the tip end effector can be represented in the configuration Cartesian coordinate:

$$X_e = [R(1 - \cos\beta) + h\sin\beta]\cos\alpha \tag{5}$$

$$Y_e = [R(1 - \cos\beta) + h\sin\beta]\sin\alpha \tag{6}$$

$$Z_e = R\sin\beta + h\cos\beta \tag{7}$$

Using MATLAB simulation, the workspace of the catheter tip is shown in Fig. 3C, where its workspace is extendable and composed of a set of concentric spheres with increasing radii and partially missing bottom areas.

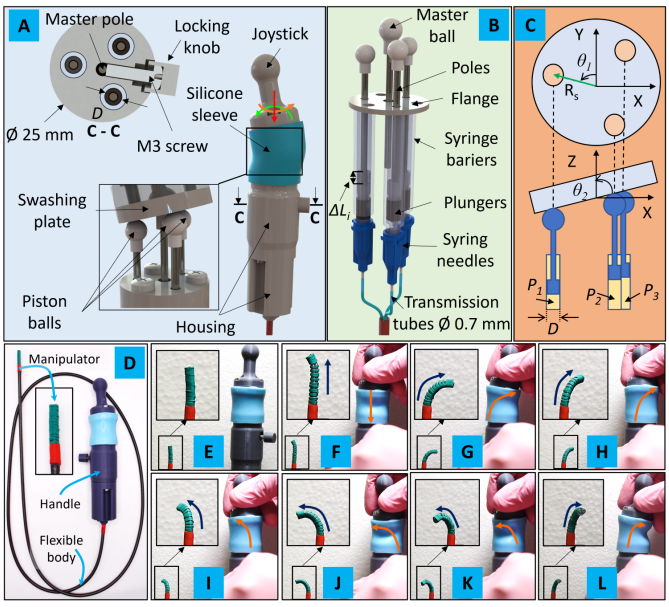

Fig. 4. The proposed handheld controller: (A) Design and working principle with cross-section C-C; (B) Inner components; (C) Kinematic model of the working principle; (D) Prototype the handle catheter device; One-to-one mapping motions: (E) Original state; (F) Elongating states; (G) - (L) Bending states.

C. Hydraulic handheld controller

To hydraulically control the soft manipulator with an intuitive interface, a handheld controller was proposed using a swash plate mechanism. Fig. 4 shows the design, working principle, and modeling of the proposed handheld controller. Three 1 ml syringes were used and arranged 120° apart, each of them had a barrier cut in half. The syringe piston was composed of a stainless-steel pole, a rubber plunger, and 3D-printed balls (Fig. 4B). These syringes were connected to the medical needles (G28), which were then connected to the long fluid transmission tubes linking to the flexible manipulator SMMs. As a result, the change in internal fluid pressure or volume would induce the manipulator motions of elongating or bending, which has been discussed above. To change the volume inside each syringe, a swashing plate was used to push the syringe piston via being contacted with the piston balls (Fig.4A). A master ball which was kept inside the swashing plate and a joystick were assembled to create a spherical joint, allowing the swashing plate to be tilted. The master ball was also linked to a stainless-steel pole to allow the swashing plate to be translated. A flange with several through holes was used to stabilize the axial movement of the poles and avoid swaying. Two 3D-printed parts were used as the housing of the handle, while a silicone sleeve was used to keep contact between the swashing plate and the piston balls. Briefly, users could hold the handle and control the flexible manipulator by simply rotating or pushing the joystick. In some cases, elongating the manipulator is required. Therefore, a locking knob with an M3 screw was used to limit the master pole translation (cross-section C-C). At this state, users could only be able to tilt the joystick to bend the flexible manipulator.

To investigate how the handheld controller drives the flexible manipulator, a model for the handle was built based on [27]. Fig. 4C shows the perpendicular projections of the swashing mechanism onto XY and XZ planes. While the Z-axis is defined as the central axis of the three cylinders, the Y-axis is the vertical axis, and the X-axis is perpendicular to the YZ plane. The displacement of the i^{th} piston $(i = 1, 2, 3)$ can be described as:

$$\Delta L_i = R_s \sin[\theta_1 + (i-1)\frac{2\pi}{3}] \cos\theta_2 + L_s \qquad (8)$$

where, R_s is the reference radius of the syringe piston, θ_1 is the azimuth angle of the swashing plate or the angle between the Y-axis and the first syringe, θ_2 is the tilted angle of the swashing plate or the angle between the swashing plate and Z axis, and L_s is the displacement of the plunger with respects to the translation along Z-axis of the swashing plate.

With D (mm) being the inner diameter of the syringe barrier, the input volume from each syringe to the SMM can be deprived as follows:

$$V_i = \frac{\pi}{4} D^2 R_s \sin[\theta_1 + (i-1)\frac{2\pi}{3}] \cos\theta_2 + L_s \qquad (9)$$

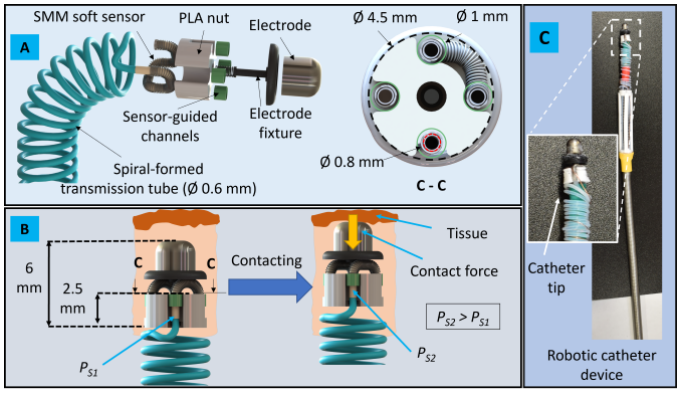

Fig. 5. The design and prototype of the catheter tip: (A) The explored assembly of the catheter tip with cross-section D-D; (B) Original and tissue contacted states of the catheter tip; (C) Overview of the catheter tip prototype.

The relationship between the liquid volume, the elongated length of the SMM, and the input pressure can be depicted as:

$$V_i P_i = \frac{1}{2}(k_c + k_r) l_i^2 + W_l \qquad (10)$$

where, $k_r = \frac{EA_{tube}L_0}{(L_0+l_i)^2}$ is the instantaneous elastic constant of the soft microtubule and W_l is the energy lost caused by the friction. Fig. 4D shows the handle prototype connected to the catheter flexible body and the manipulator.

D. Soft force sensor

In this work, we also introduced a novel concept of a soft force sensor based on the change of hydraulic pressure, enabling a high-sensitivity and low-cost solution. Figs. 5A and B depict the design of a catheter tip, where a soft sensor was wound on the top surface of a 3D-printed-PLA nut. The soft sensor was made of a Ø0.8 x 8 mm SMM connected to a Ø0.6 mm long transmission tube. This SMM was initially pressurized to reach an inner pressure of P_{S1} and was then threaded through four sensor-guided channels forming two bending curves, which directly contact the bottom surface of an electrode fixture (or ablation electrode). When the ablation electrode was contacted with the tissue, a force acting on two curves caused an increase in the internal pressure of the soft sensor to $P_{S2} > P_{S1}$. This change ($\Delta P = P_{S2} - P_{S1}$) could be processed to represent tool-tissue-interacting feedback information (Fig. 5B). The hydraulic pressure was externally monitored by commercial hydraulic pressure. It is worth noting that the fluid transmission tube plays a keystone to transmit fluid pressure at any distance and length, making it a well-suited method for a flexible surgical system. In the original state, the overall diameter and the height of the catheter tip were 4.5 mm and 6 mm, respectively. Since the catheter tip would be attached to the flexible manipulator, the fluid transmission tube was designed with a spiral shape in order to mitigate unexpected effects on the manipulator's bending motion. Fig. 5C illustrates the catheter tip prototype

where the soft force sensor was attached to the flexible manipulator.

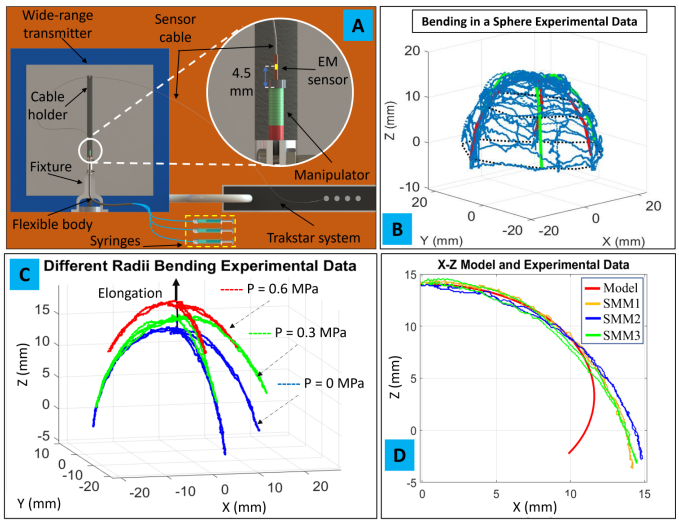

Fig. 6. (A) Experimental setup for the workspace analysis of the manipulator; (B) Experimental data for bending motion of the manipulator on a spherical surface; (C) Bending motion of the manipulator when one SMM was activated, and the other two were kept at pressures of P_f = (0, 0.3, 0.6) MPa represented by blue, green, and red colors, respectively; (D) Comparison between the model and experimental data in the XZ plane.

III. Experimental Chracterizations

A. Workspace analysis and device validation

The workspace of the catheter was characterized using an electromagnetic magnetic (EM) tracking system (TRACKLAB – FREEDSPACE Ltd, Canada), an independent measurement. We used an EM 6-DOFs sensor (model 90) which was attached to the top surface of the flexible manipulator to record the catheter tip (Fig. 6A). It is noted that the distance from the core of the EM sensor to the manipulator end was equal to that from the end-effector (h = 4.5 mm) (see Fig. 2B). Additionally, the EM sensor cable was hung up by a holder to minimize its effect on the manipulator movement. The manipulator was steered to create a sphere within a predetermined input pressure range of [0, 0.6] MPa. Fig. 6B describes the collected data from this experimental step, confirming that the end-effector could move on a spherical surface.

To verify if the end-effector could reach different radii spheres without moving the catheter body as proposed in Fig. 3, a second experiment was conducted. While one SMM was constantly activated in the range of P_a = [0, 0.6] MPa, the other two SMMs were simultaneously pressurized and kept at three different pressures P_f = (0, 0.3, and 0.6) MPa . The results of this experiment are illustrated in Fig. 6C, showing that the end-effector could move on various spherical surfaces with increasing radii when the input pressure was increased. The experimental data with P_f = 0 MPa were converted into 2D (XZ plane) to compare with its mathematical model. In the range of X = [0, 11.5] mm, the results revealed a similarity between the experimental data and the model. Errors start increasing at $X \approx 11.5$ mm and became progressively apparent. This can be explained by the influence of the EM sensor cable on the manipulator's movement, which prevented it from bending inward. In future work, a wireless magnetic tracking system or optical tracking system should be used.

We also validate the mapping capability between the handheld controller and the flexible bending manipulator in the same frame using a Nikon D3500 HD camera (Nikon Inc., Japan). Figs. 4E, F, and G to L respectively present the original, elongating, and bending states of the flexible manipulator corresponding with the movement of the handle joystick manipulated by a hand. The results confirmed that our developed hand-held controller could precisely map the motion from the user input to the bending motion of the flexible manipulator.

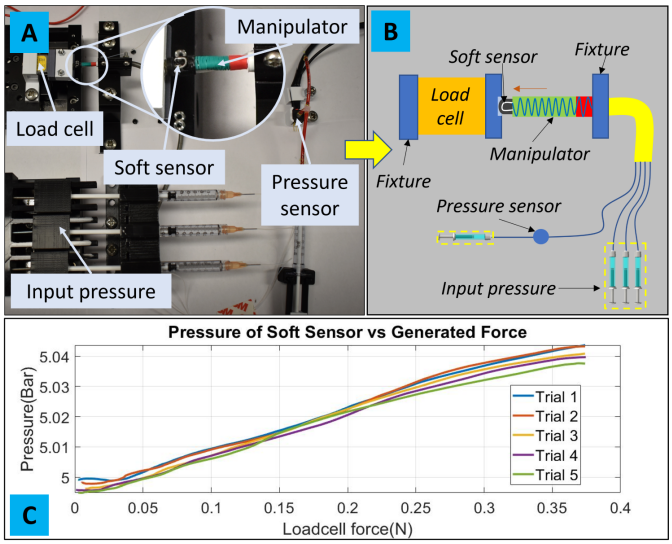

Fig. 7. (A) Setup for force sensing characterization of the soft sensor. (B) Schematic of the experimental implementation. (C) Experimental data of the soft sensor versus the generated force sensed by the load cell.

B. Force sensing characterization of the soft sensor

To validate the sensing capability of the developed soft sensor when it was integrated into the tip of the flexible manipulator, an experimental set-up was built as shown in Fig. 7A. The flexible manipulator was hydraulically driven by a set of three syringes with the same initial pressure. A commercial pressure sensor (model 40PC250G2A, Honeywell, USA) was connected to the soft sensor, and a syringe was used to record the pressure change of the soft sensor. It is noted that the soft sensor was initially pressurized to reach P_{S1} = 5 Bars. A load cell (model LSB200, FUTEK, USA) was used to monitor the interaction force, which was then used to compare with the soft sensor signals. When the three syringes were pressurized, the manipulator would be elongated to push the catheter tip against the load cell. This action was repeated five times during the experiment.

Experimental results revealed that the soft sensor could sense a contact force (Fig. 7C) ranging from 0 to 0.375 (N) within the required range of 0.2 to 0.3 N for normal cardiac ablation procedures [2]. In addition, it is straightforward to calculate the sensitivity (or gauge factor (GF)) of the new sensor by measuring the slope of the hydraulic pressure-force curve, which was around 10.7 kPa/N. This result also confirmed that the GF of the sensor is relatively high compared to commercial strain gauges or force sensors.

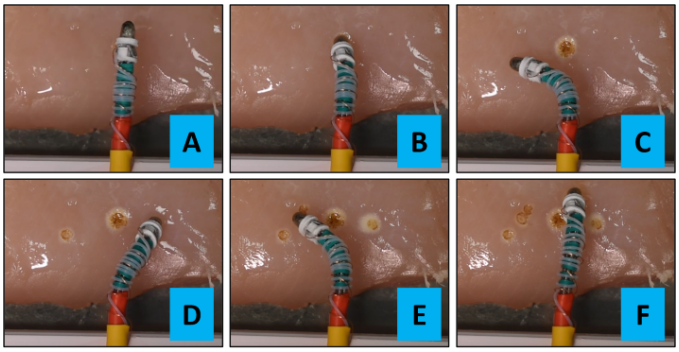

Fig. 8. The ablation experimental results of the catheter tip: (A) Original position; (B)-(F) Ablation positions.

C. $Ex-vivo$ experiment

To validate our developed catheter system, we also conducted an additional $ex-vivo$ ablation procedure on fresh porcine tissue where the ablation electrode of the catheter was directly connected to an electrosurgical unit (Led Surtron 120, Stark Medical Australia Pty Ltd). During the validation, the catheter tip was steered to reach different workspaces (different radii) while performing the ablation. The exposed area of the ablated tissue is shown in Fig. 8. These results demonstrated that our developed catheter system could be potentially used to perform cardiac ablation with extendable working space without moving the catheter body, avoiding complex translation motion which is normally associated with nonlinear backlash and complex motion control.

IV. Discussion and Conclusion

A handheld soft robotic catheter with bending, extending, and sensing capability and an ergonomic handle was developed for the treatment of AF and other arrhythmias including supra-ventricular tachycardias. The flexible manipulator of the soft catheter was successfully fabricated using three SMMs, which could induce omnidirectional bending motions and workspace extension without the need of moving the catheter body. This feature enabled the catheter the ability to reach dexterous and complex paths of the blood vessels and also within the internal chambers of the heart. This manipulator was hydraulically controlled by a novel ergonomic handle with a swashing mechanism and a fit-in-hand size, enabling intuitive control and compactness. This new design is expected to reduce significant training time for novices as well as installation time which is well-suited for emergency cardiac surgeries.

The workspace and the handheld controller of the catheter system were modeled and validated with a magnetic tracking system. Experimental results revealed that the workspace of the catheter tip can be predicted based on the kinematic models and a set of concentric spheres with increasing radii. Meanwhile, the handheld controller was able to map one by one the bending motion of the handle to the 3D motion of the flexible manipulator.

The use of the SMM enabled the catheter system with the capability of generating sufficient force (at least 0.375 N) which is more than sufficient for a cardiac ablation procedure. To sense the interaction force between the catheter tip and the tissue for safe operation, a novel soft hydraulic sensor was developed. The soft sensor was characterized to sense the contact force generated by the manipulator against contacting objects. The validated results also showed that the new soft sensor had a high sensitivity of about 10.7 kPa/N, and most importantly, it can able to sense the required range of ablation force from 0.2 to 0.3 N [2]. $Ex-vivo$ experiments were also carried out to validate the feasibility of the device to be used for cardiac ablation surgery. In future clinical trials, the catheter design will be modified to include a silicone layer that will protect the electrical wiring and prevent exposure, thereby avoiding tissue damage.

In conclusion, the developed soft robotic catheter device showed great potential to be used for cardiac ablation procedures with a sufficiency of fundamental functions. In addition, it also has the potential to be scaled and extended for use in other flexible surgical applications such as endoscopic surgery or areas related to natural orifice transluminal endoscopic surgery (NOTES).

Acknowledgment

Chi Cong Nguyen, Mai Thanh Thai, and Trung Thien Hoang would like to thank the support of the Science and Technology scholarship Program for Overseas Study for Master's and Ph.D. degrees, VinUniversity, Vingroup, Vietnam.

References

[1] G. Bassil, S. M. Markowitz, C. F. Liu, G. Thomas, J. E. Ip, B. B. Lerman, and J. W. Cheung, "Robotics for catheter ablation of cardiac arrhythmias: current technologies and practical approaches," *Journal of Cardiovascular Electrophysiology*, vol. 31, no. 3, pp. 739–752, 2020.

[2] D. Padmanabhan, P. S. M. Rao, and H. J. Pandya, "Force sensing technologies for catheter ablation procedures," *Mechatronics*, vol. 64, p. 102295, 2019.

[3] L. Rottner, B. Bellmann, T. Lin, B. Reissmann, T. Tönnis, R. Schleberger, M. Nies, C. Jungen, L. Dinshaw, and N. Klatt, "Catheter ablation of atrial fibrillation: state of the art and future perspectives," *Cardiology and Therapy*, vol. 9, no. 1, pp. 45–58, 2020.

[4] C. C. Nguyen, S. Wong, M. T. Thai, T. T. Hoang, P. T. Phan, J. Davies, L. Wu, D. Tsai, H.-P. Phan, N. H. Lovell, and T. N. Do, "Advanced user interfaces for teleoperated surgical robotic systems," *Advanced Sensor Research*, vol. n/a, no. n/a, p. 2200036, 2023. [Online]. Available: https://onlinelibrary.wiley.com/doi/abs/10.1002/adsr.202200036

[5] P. Kanagaratnam, M. Koa-Wing, D. T. Wallace, A. S. Goldenberg, N. S. Peters, and D. W. Davies, "Experience of robotic catheter ablation in humans using a novel remotely steerable catheter sheath," *Journal of Interventional Cardiac Electrophysiology*, vol. 21, no. 1, pp. 19–26, 2008.

[6] H. M. Le, T. N. Do, and S. J. Phee, "A survey on actuators-driven surgical robots," *Sensors and Actuators A: Physical*, vol. 247, pp. 323–354, 2016.

[7] J. Lussi, M. Mattmann, S. Sevim, F. Grigis, C. De Marco, C. Chautems, S. Pané, J. Puigmartí-Luis, Q. Boehler, and B. J. Nelson, "A submillimeter continuous variable stiffness catheter for compliance control," *Advanced Science*, vol. 8, no. 18, p. 2101290, 2021.

[8] J. Hwang, J.-y. Kim, and H. Choi, "A review of magnetic actuation systems and magnetically actuated guidewire-and catheter-based microrobots for vascular interventions," *Intelligent Service Robotics*, vol. 13, no. 1, pp. 1–14, 2020.

[9] M. T. Thai, P. T. Phan, T. T. Hoang, S. Wong, N. H. Lovell, and T. N. Do, "Advanced intelligent systems for surgical robotics," *Advanced Intelligent Systems*, vol. 2, no. 8, 2020.

[10] P. T. Phan, M. T. Thai, T. T. Hoang, N. H. Lovell, and T. N. Do, "Hfam: soft hydraulic filament artificial muscles for flexible robotic applications," *IEEE Access*, vol. 8, pp. 226 637–226 652, 2020.

[11] M. T. Thai, P. T. Phan, T. T. Hoang, H. Low, N. H. Lovell, and T. N. Do, "Design, fabrication, and hysteresis modeling of soft microtubule artificial muscle (smam) for medical applications," *IEEE Robotics and Automation Letters*, vol. 6, no. 3, pp. 5089–5096, 2021.

[12] M. Cianchetti, C. Laschi, A. Menciassi, and P. Dario, "Biomedical applications of soft robotics," *Nature Reviews Materials*, vol. 3, no. 6, pp. 143–153, 2018.

[13] C. C. Nguyen, T. Teh, M. T. Thai, P. T. Phan, T. T. Hoang, H. Low, J. Davies, E. Nicotra, N. H. Lovell, and T. N. Do, "Bidirectional soft robotic catheter for arrhythmia treatment," in *2022 International Conference on Robotics and Automation (ICRA)*. IEEE, Conference Proceedings, pp. 9579–9585.

[14] P. T. Phan, T. T. Hoang, M. T. Thai, H. Low, N. H. Lovell, and T. N. Do, "Twisting and braiding fluid-driven soft artificial muscle fibers for robotic applications," *Soft Robotics*, vol. 9, no. 4, pp. 820–836, 2022.

[15] P. Polygerinos, A. Ataollahi, T. Schaeffter, R. Razavi, L. D. Seneviratne, and K. Althoefer, "Mri-compatible intensity-modulated force sensor for cardiac catheterization procedures," *IEEE Transactions on Biomedical Engineering*, vol. 58, no. 3, pp. 721–726, 2010.

[16] H. J. Pandya, K. Park, and J. P. Desai, "Design and fabrication of a flexible mems-based electro-mechanical sensor array for breast cancer diagnosis," *Journal of Micromechanics and Microengineering*, vol. 25, no. 7, p. 075025, 2015.

[17] N. Thanh-Vinh, N. Binh-Khiem, H. Takahashi, K. Matsumoto, and I. Shimoyama, "High-sensitivity triaxial tactile sensor with elastic microstructures pressing on piezoresistive cantilevers," *Sensors and Actuators A: Physical*, vol. 215, pp. 167–175, 2014.

[18] K. Yokoyama, H. Nakagawa, D. C. Shah, H. Lambert, G. Leo, N. Aeby, A. Ikeda, J. V. Pitha, T. Sharma, and R. Lazzara, "Novel contact force sensor incorporated in irrigated radiofrequency ablation catheter predicts lesion size and incidence of steam pop and thrombus," *Circulation: Arrhythmia and Electrophysiology*, vol. 1, no. 5, pp. 354–362, 2008.

[19] H. Wang and H. Cao, "Irrigated ablation catheter having a pressure sensor to detect tissue contact, us patent 7,591,816, 2009," 2009.

[20] T. T. Hoang, P. T. Phan, M. T. Thai, N. H. Lovell, and T. N. Do, "Bio-inspired conformable and helical soft fabric gripper with variable stiffness and touch sensing," *Advanced Materials Technologies*, vol. 5, no. 12, p. 2000724, 2020.

[21] H. Nakagawa, J. Kautzner, A. Natale, P. Peichl, R. Cihak, D. Wichterle, A. Ikeda, P. Santangeli, L. Di Biase, and W. M. Jackman, "Locations of high contact force during left atrial mapping in atrial fibrillation patients: electrogram amplitude and impedance are poor predictors of electrode-tissue contact force for ablation of atrial fibrillation," *Circulation: Arrhythmia and Electrophysiology*, vol. 6, no. 4, pp. 746–753, 2013.

[22] P. Valdastri, K. Harada, A. Menciassi, L. Beccai, C. Stefanini, M. Fujie, and P. Dario, "Integration of a miniaturised triaxial force sensor in a minimally invasive surgical tool," *IEEE Transactions on Biomedical Engineering*, vol. 53, no. 11, pp. 2397–2400, 2006.

[23] F. Focacci, M. Piccigallo, O. Tonet, G. Megali, A. Pietrabissa, and P. Dario, "Lightweight hand-held robot for laparoscopic surgery," in *Proceedings 2007 IEEE International Conference on Robotics and Automation*. IEEE, Conference Proceedings, pp. 599–604.

[24] J. Shang, D. P. Noonan, C. Payne, J. Clark, M. H. Sodergren, A. Darzi, and G.-Z. Yang, "An articulated universal joint based flexible access robot for minimally invasive surgery," in *2011 IEEE International Conference on Robotics and Automation*. IEEE, Conference Proceedings, pp. 1147–1152.

[25] D. Gelman, A. C. Skanes, M. A. Tavallaei, and M. Drangova, "Design and evaluation of a catheter contact-force controller for cardiac ablation therapy," *IEEE Transactions on Biomedical Engineering*, vol. 63, no. 11, pp. 2301–2307, 2016.

[26] M. T. Thai, T. T. Hoang, P. T. Phan, N. H. Lovell, and T. N. Do, "Soft microtubule muscle-driven 3-axis skin-stretch haptic devices," *IEEE Access*, vol. 8, pp. 157 878–157 891, 2020.

[27] T. Wang, Y. Zhang, Z. Zhu, and S. Zhu, "An electrohydraulic control device with decoupling effect for three-chamber soft actuators," *IEEE/ASME Transactions on Mechatronics*, 2021.